RAPID COMMUNICATIONS

PHYSICAL REVIEW B VOLUME 52, NUMBER 20 15 NOVEMBER 1995-II

Subpicosecond hole tunneling by nonresonant delocalization in asymmetric double quantum wells

M. F. Krol
Rome Laboratory Photonics Center, Griffiss Air Force Base, New York 13441-4515

S. Ten and B. P. McGinnis
Optical Sciences Center, University of Arizona, Tucson, Arizona 85721

M. J. Hayduk
Rome Laboratory Photonics Center, Griffiss Air Force Base, New York 13441-4515

G. Khitrova and N. Peyghambarian
Optical Sciences Center, University of Arizona, Tucson, Arizona 85721

(Received 5 July 1995)

We present experimental evidence for subpicosecond hole tunneling in asymmetric double-quantum-well structures. A single tunneling time is observed at low carrier densities indicating that hole tunneling times are at least as fast as electron tunneling times despite the absence of resonances between hole states. We have conducted band-structure and tunneling-time calculations suggesting that nonresonant delocalization of hole wave functions combined with alloy scattering provides an efficient mechanism for fast hole transfer from the narrow well (NW) to the wide well (WW) at finite in-plane momenta. We suggest that holes tunnel to the WW before reaching the bottom of the lowest subband in the NW.

Recently, a tunneling mechanism was predicted by Goldoni and Fasolino which does not rely on resonances to facilitate hole tunneling in asymmetric double-quantum-well- (ADQW) structures.[1] Since ADQW's lack inversion symmetry, the Kramers degeneracy is lifted causing spin splittings to appear in the valence-band structure. In momentum regions where spin splitting is enhanced due to the proximity of other bands, a concomitant nonresonant delocalization of the hole wave function appears. This nonresonant delocalization provides a mechanism for ultrafast hole tunneling which has, until now, not been observed experimentally. It has been noted that electrons may tunnel rapidly via longitudinal optical (LO) phonon scattering when the energy separation between the lowest energy level in the narrow well (NW) and the lowest energy level in the wide well (WW) is larger than the LO phonon energy.[2–5] Fast hole tunneling between the NW and WW may also occur when there are resonances between hole subbands due to the presence of an applied electric field[6,7] or due to valence-band mixing between NW and WW subbands.[8,9]

In this paper, we present experimental evidence for subpicosecond hole tunneling in ADQW structures even though there is an absence of resonances between hole states. The study utilized the ternary $Ga_{0.47}In_{0.53}As/Al_{0.48}In_{0.52}As$ system instead of the commonly studied $GaAs/Al_xGa_{1-x}As$ system. The $Ga_{0.47}In_{0.53}As$ system is ideal for studying hole tunneling in ADQW's since the light-hole effective mass is half that of GaAs and results in increased delocalization of the hole wave functions over the ADQW structure.[10] Our band-structure and tunneling-time calculations indicate that scattering due to the randomly fluctuating alloy potential combined with nonresonant delocalization is an efficient mechanism for rapid hole transfer from the NW to the WW at finite in-plane momenta. In particular, our results indicate that holes tunnel to the WW before reaching the bottom of the lowest subband in the NW.

The ADQW samples studied consisted of 30 periods of the following structure: 40-Å $Ga_{0.47}In_{0.53}As$ well/L_b-Å $Al_{0.48}In_{0.52}As$ tunnel barrier/60-Å $Ga_{0.47}In_{0.53}As$ well/150-Å $Al_{0.48}In_{0.52}As$ barrier, where L_b is the thickness of the tunnel barrier. These structures were grown by solid-source molecular-beam epitaxy on semi-insulating (100) InP substrates. Three samples were studied with barrier widths of $L_b = 27$, 37, and 100 Å, denoted later as $40/L_b/60$. The well widths were chosen such that at 77 K the NW and WW heavy-hole exciton transition wavelengths were near 1.23 and 1.34 μm, respectively. The samples were of high quality as indicated by low-temperature linear absorption [see inset of Fig. 1(b)] and photoluminescence measurements. The sample with the 100-Å barrier has essentially decoupled wells and experimentally shows no effects due to tunneling. The ADQW samples were designed such that the energy separation between the lowest electron energy levels in the WW and NW was approximately 61 meV (the separation increased slightly as the barrier width was decreased). A large separation between the levels was chosen for two reasons: first, for energy separations less than 50 meV the calculated electron tunneling times were subpicosecond, making the pump-induced transmission changes difficult to observe experimentally; and second, the separation between the levels is far from being in resonance with the LO phonon energy, hence avoiding any significant change in the electron tunneling time due to space-charge-induced level shifts.

The experimental system used to measure the carrier dynamics utilized a time-resolved transmission/up-conversion technique. In most previous studies of carrier dynamics in ADQW's, time-resolved photoluminescence (PL) was utilized. In time-resolved PL, the product $f_e f_h$ is measured,

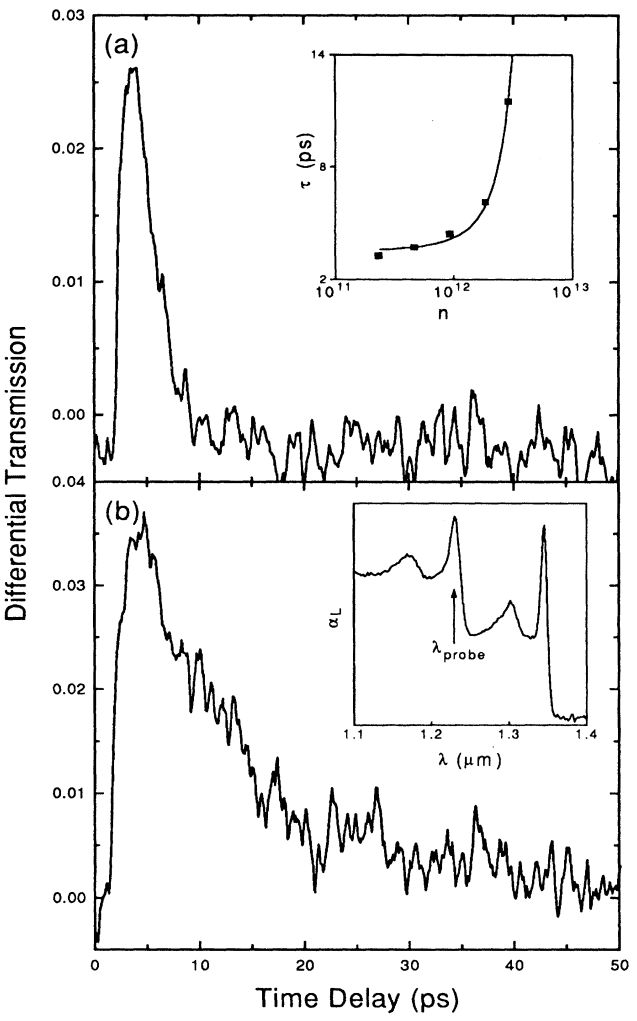

FIG. 1. (a) Time-resolved differential transmission data for sample 40/27/60 at a carrier density of 1.4×10^{11} cm^{-2}. The inset shows the carrier-density dependence of the fast recovery component of the data shown in the figure (squares) and the calculated electron tunneling time (solid line). (b) Time-resolved differential transmission data for sample 40/37/60 at the same carrier density as in (a). The inset shows a typical 77-K linear absorption spectrum of the samples.

where f_e and f_h are the Fermi distributions of the electrons and holes, respectively. Hence, if one type of carrier is absent, the total signal is zero despite the existence of the other carrier. On the other hand, transmission techniques measure $1\text{-}f_e\text{-}f_h$. Therefore, the dynamics of the individual carriers change the transmission signal independently. In our approach, 100-fs pulses at 844 nm from a mode-locked Ti:sapphire laser were used to pump the samples and provide reference pulses for the up-conversion process. The photon energy of the pump was tuned to generate carriers only in the wells, not in the barriers, with most of the excess energy carried by the electrons. A continuous-wave Cr:forsterite laser provided a tunable probe from 1.22 to 1.29 μm. The probe laser was tuned to the heavy-hole exciton absorption resonance of the NW for all measurements discussed in this paper [see inset of Fig. 1(b)]. The samples were held at 77 K in a liquid-nitrogen cryostat. The transmitted probe was mixed with the reference pulses in a $LiIO_3$ crystal to provide femtosecond time resolution. The temporal resolution of the system was 220 fs and was limited by the group-velocity mismatch between the reference and probe in the nonlinear crystal. The up-converted photons were spectrally filtered and then detected by a photomultiplier tube. The pump was chopped to measure the pump-induced changes in the transmitted probe using lock-in detection.

The time-resolved transmission data for sample 40/27/60 is shown in Fig. 1(a) for a carrier density of 1.4×10^{11} cm^{-2}. Of these carriers approximately 3.5×10^{10} cm^{-2} were generated in the NW with the remaining 1.05×10^{11} cm^{-2} being generated in the WW. The difference in carrier densities between the two wells stems from the larger WW width (1.5 times larger than the NW) and the existence of two allowed WW interband transitions at the pump energy as opposed to one in the NW. The initial rise shows the relaxation of carriers to the bottom of the NW band. The subsequent decay is due to tunneling of carriers from the NW to the WW. A striking feature in this data is the fast and full recovery of the transmission at this carrier density. The decay was fitted to a *single* exponential decay constant of 2.4 ps. The transmission fully recovers with a single time constant despite the fact that the probe wavelength was tuned to the heavy-hole exciton absorption peak of the NW. Since the up-conversion technique measures $1\text{-}f_e\text{-}f_h$, full recovery indicates the absence of both electron and hole populations. At high carrier densities a two-component decay can be seen with a long-lasting component being present. To verify that the fast component of the decay was associated with the tunneling of carriers from the NW to the WW, the same measurements were performed using sample 40/37/60. The measured differential transmission signal is shown in Fig. 1(b). The time constant associated with the decay was 11.5 ps. The results are consistent with tunneling phenomena, i.e., for a thicker barrier the time constant of the fast component becomes longer. Sample 40/100/60 showed no recovery over our delay range, consistent with an essentially decoupled pair of wells.

To understand the dynamics observed in this work, we first considered the electron behavior independently of the holes. Since the interwell dynamics are not significantly affected by excitonic effects,[11] we have neglected the Coulomb attraction between electrons and holes in the following calculations. To model the electron dynamics we employed the LO phonon-scattering model developed by Price.[12] The model utilizes Fermi's golden rule and assumes bulk phonon modes. The LO phonon energy for the $Ga_{0.47}In_{0.53}As$ well material was assumed to be 33.2 meV.[13] To include the effects of band filling on the electron tunneling times, the ordinary density of final states in the wide well $g_{WW}(E)$ was replaced by $[1-f_{WW}(E,T_c)]g_{WW}(E)$, where $f_{WW}(E,T_c)$ is the Fermi distribution of electrons in the wide well, E is the electron energy relative to the bottom of the bulk $Ga_xIn_{1-x}As$ conduction band, and T_c is the carrier temperature. The effect of alloy scattering was also considered theoretically; however, the calculated tunneling times were two orders of magnitude longer than the LO phonon-assisted tunneling times.

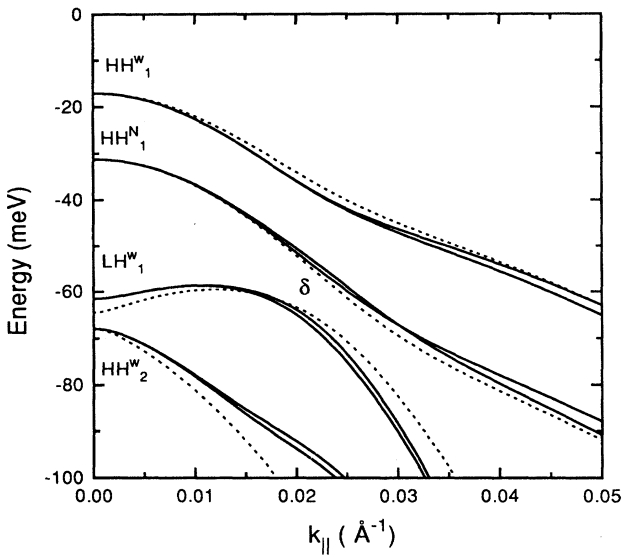

FIG. 2. Valence-band dispersion for the first four subbands of the 40/27/60 ADQW structure (solid lines). The valence-band dispersion for the isolated 40- and 60-Å quantum wells is also shown (dashed lines). The labels at $k_{\|}=0$ indicate the character of the bands at the Γ point.

At low carrier densities the calculated electron tunneling times for samples 40/27/60 and 40/37/60 are 2.4 and 10.5 ps, respectively. These times are in good agreement with the measured low-density decay times. Thus, the transmission *fully recovers* with a time constant equal to the electron tunneling time. The inset of Fig. 1(a) shows the measured carrier-density dependence of the fast recovery component for sample 40/27/60 and the calculated carrier-density dependence of the electron tunneling time (solid line). The tunneling times increase as the carrier density is increased, consistent with band filling in the WW acting as a blocking mechanism to tunneling electrons. The calculated tunneling times fit the measured data best using a carrier temperature of 150 K, indicating that the electron distributions are still hot during the tunneling process.[4] The good agreement between the observed fast recovery and the calculated electron tunneling time indicates that at low carrier densities the holes must tunnel as fast as, or faster than, the electrons. For lower carrier densities, the observed dynamics is not expected to change significantly since at the carrier densities in question, space-charge and phase-space filling effects are already negligible.

To investigate hole tunneling in the low-carrier-density limit, we calculated the valence-band structure for our ADQW samples. To include the effects of band mixing, the 4×4 Luttinger Hamiltonian with angular momentum quantized parallel to the growth axis was solved using a method similar to that outlined in Ref. 14. The hole dispersion of the first four subbands of the 40/27/60 ADQW structure is shown in Fig. 2. The bands are labeled by their character at the Γ point. The dispersion relations for the isolated single 40 and 60-Å quantum wells are shown as dashed lines. We probe the holes at the Γ point of the first heavy-hole band of the NW, labeled HH_1^N. Immediately obvious is the absence of any crossings between subbands of the isolated quantum wells. Hence, holes created with large in-plane momenta, as in this case, do not have a resonant mechanism for fast hole tunneling from the NW to the WW. The band structure of the second (HH_1^N) and third (LH_1^W) subbands shows two very interesting features in the region of $k_{\|}\approx 0.015$ Å^{-1}, labeled δ. The hole wave functions of both bands are strongly delocalized in this momentum region and have no definite parity as found by Goldoni and Fasolino;[1] and the third subband, LH_1^W, has a local maximum at $k_{\|}\approx 0.01$ Å^{-1}. Hence, the density of states there is expected to be very large (in principle infinite). To elucidate the contribution of these features to the tunneling process, the tunneling rates were estimated under the Born approximation by using the Fermi golden rule. After summing over all possible final states,

$$\frac{1}{\tau}=\frac{S}{2\pi\hbar}\{k'/|d\varepsilon/dk'|\}\int_0^{2\pi}d\theta|\langle\vartheta_{k'}(\mathbf{r})|V_q(\mathbf{r},q)|\vartheta_k(\mathbf{r})\rangle|^2, \tag{1}$$

where $\vartheta_k(\mathbf{r})$ and $\vartheta_{k'}(\mathbf{r})$ denote the initial and final state 4×1 spinors in the growth direction, $V_q(\mathbf{r},q)$ is a general scattering potential, S is the sample area, $q^2=k^2+k'^2-2kk'\cos\theta$, and θ is the angle in k space.

For disordered alloys such as $Ga_xIn_{1-x}As$ and $Al_xIn_{1-x}As$, intersubband transitions will be dominated by alloy scattering;[15] hence the scattering potential in Eq. (1) becomes

$$V_{\text{alloy}}(\mathbf{r})=I\Omega_0\langle\delta V\rangle\left[\sum_{\mathbf{R}_B}x\,\delta(\mathbf{r}-\mathbf{R}_b)-\sum_{\mathbf{R}_A}(1-x)\,\delta(\mathbf{r}-\mathbf{R}_A)\right], \tag{2}$$

where Ω_0 is the volume of the alloy unit cell, $\langle\delta V\rangle$ is the spatial average of the fluctuating alloy potential over the alloy unit cell, I is the 4×4 identity matrix, x is the A mole fraction in the ternary alloy $A_xB_{1-x}C$, and R_i ($i=A$ or B) is the spatial position of the scattering site. By inserting Eq. (2) into Eq. (1) and averaging the squared modulus of the matrix element over the volume of the disordered alloy,[14] we obtain

$$\frac{1}{t}=\frac{\Omega_0}{\hbar}\langle\delta V\rangle^2x(1-x)\{k'/|d\varepsilon/dk'|\}\int|\vartheta_{k'}(z)|^2|\vartheta_k(z)|^2dz. \tag{3}$$

Since Eq. (3) is independent of q due to the short-range nature of $V_{\text{alloy}}(\mathbf{r})$, the tunneling rate is directly proportional to the overlap integral of the probability densities in the growth direction and the density of final states. Figure 3 shows the spin-conserving tunneling time dependence on initial-state momentum $k_{\|}$ for transitions from HH_1^N to HH_1^W (solid line) and LH_1^W (dashed line). For $Ga_{0.47}In_{0.53}As/Al_{0.48}In_{0.52}As$ heterostructures we assumed $x=0.47$, $d=5.8688$ Å ($\Omega_0=d^3/4$), and $\langle\delta V\rangle=1.3$ eV.[16] The dominant feature seen in Fig. 3 is the strong dependence of tunneling time on the initial-state momentum, i.e., upon band mixing. In particular, the tunneling times are subpicosecond over a wide range of $k_{\|}$. As expected from Eq. (3), the tunneling times from HH_1^N to LH_1^W approach zero (infinite rate) as the initial-state energy approaches the energy at which LH_1^W goes through a local maximum. The tunneling times from HH_1^N to HH_1^W are also short in the region of

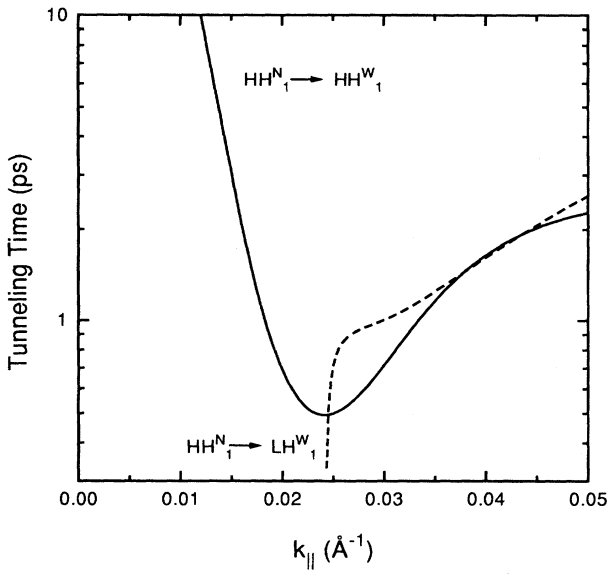

FIG. 3. Calculated dependence of the hole tunneling time on initial-state in-plane momentum due to alloy scattering. Tunneling times from HH_1^N to HH_1^W (solid line) and LH_1^W (dashed line) are shown.

$k_\parallel \approx 0.025$ Å^{-1}. The delocalization of these hole wave functions is enhanced in this momentum region due to band mixing and the proximity of LH_1^W. The overlap of the probability densities of HH_1^N and HH_1^W is therefore increased. Thus, we conclude that in disordered alloys, holes with finite $k_\parallel$ can tunnel from the NW to the WW on subpicosecond time scales.

The results of the preceding analysis can be used to qualitatively explain the time-resolved data at low carrier density shown in Fig. 1. The full recovery of the transmission implies that both the electrons and the holes tunnel with at least picosecond speeds. However, the hole tunneling time at the Γ point (see Fig. 3) is at least an order of magnitude larger than the experimentally observed times. Since holes are generated in the HH_1^N subband with significant excess energy by the pump pulse, i.e., at $k_\parallel \approx 0.05$ Å^{-1}, at low carrier densities the holes must tunnel from the NW to the WW *before* relaxing to the bottom of HH_1^N. On the other hand, at high carrier densities the hole states at the bottom of HH_1^W become filled and block tunneling holes. The rates of tunneling to the WW and relaxation in the NW become comparable in this case, and as a result, holes are scattered to the bottom of HH_1^N generating the long-lasting component of the differential transmission signal.

In conclusion, we have presented experimental evidence for subpicosecond hole tunneling by nonresonant delocalization and alloy scattering in ternary ADQW's. The full recovery of the differential transmission signal at low carrier densities is described in terms of holes tunneling to the WW on subpicosecond time scales before reaching the bottom of the lowest subband in the NW.

We would like to thank Dr. H. M. Gibbs for many fruitful discussions. We acknowledge support from the Rome Laboratory Photonics Center and the Optoelectronic Material Center funded through ARPA.

[1] G. Goldoni and A. Fasolino, Phys. Rev. Lett. **69**, 2567 (1992).
[2] J. Shah, in *Optics of Semiconductor Nanostructures* (Akademie Verlag, Berlin, 1993), p. 149.
[3] M. G. W. Alexander, W. W. Rühle, R. Sauer, and W. T. Tsang, Appl. Phys. Lett. **55**, 885 (1989).
[4] B. Deveaud, A. Chomette, F. Clerot, P. Auvray, A. Regreny, R. Ferreira, and G. Bastard, Phys. Rev. B **42**, 7021 (1990).
[5] A. Tacheuchi, S. Muto, T. Inata, and T. Fujii, Appl. Phys. Lett. **58**, 1670 (1991).
[6] R. Ferreira and G. Bastard, Europhys. Lett. **10**, 279 (1989).
[7] T. B. Norris, N. Vodjdani, B. Vinter, E. Costard, and E. Böckenhoff, Phys. Rev. B **43**, 1867 (1991).
[8] Ph. Roussignol, A. Vinattieri, L. Carraresi, M. Colocci, and A. Fasolino, Phys. Rev. B **44**, 8873 (1991).
[9] C. Tanguy, B. Deveaud, A. Regreny, D. Hulin, and A. Antonetti, Appl. Phys. Lett. **58**, 1283 (1991).
[10] R. P. Leavitt, J. W. Little, and S. C. Horst, Phys. Rev. B **40**, 4183 (1989).
[11] R. Strobel, R. Eccleston, J. Kuhl, and K. Köhler, Phys. Rev. B **43**, 12 564 (1991).
[12] P. J. Price, Ann. Phys. (N.Y.) **133**, 217 (1981).
[13] R. P. Leavitt and J. L. Bradshaw, J. Appl. Phys. **76**, 3429 (1994).
[14] G. Bastard, *Wave Mechanics Applied to Semiconductor Heterostructures* (Halsted, New York, 1988), p. 101.
[15] R. Ferreira and G. Bastard, Phys. Rev. B **43**, 9687 (1991).
[16] S. Mukhopahyay and B. R. Nag, Appl. Phys. Lett. **60**, 2897 (1992).